Published as: *Nat Neurosci*. 2010 January ; 13(1): .

Dissecting differential gene expression within the circadian neuronal circuit of *Drosophila*

Emi Nagoshi[1,2,4], **Ken Sugino**[2], **Ela Kula**[1,2,4], **Etsuko Okazaki**[3], **Taro Tachibana**[3], **Sacha Nelson**[2], and **Michael Rosbash**[1,2]

[1]Howard Hughes Medical Institute, Brandeis University, Waltham, Massachusetts, USA

[2]National Center for Behavioral Genomics, Department of Biology, Brandeis University, Waltham, Massachusetts, USA

[3]Department of Bioengineering, Graduate School of Engineering, Osaka City University, Osaka, Japan

Abstract

Behavioral circadian rhythms are controlled by a neuronal circuit consisting of diverse neuronal subgroups. To understand the molecular mechanisms underlying the roles of neuronal subgroups within the *Drosophila* circadian circuit, we used cell-type specific gene-expression profiling and identified a large number of genes specifically expressed in all clock neurons or in two important subgroups. Moreover, we identified and characterized two circadian genes, which are expressed specifically in subsets of clock cells and affect different aspects of rhythms. The transcription factor *Fer2* is expressed in ventral lateral neurons; it is required for the specification of lateral neurons and therefore their ability to drive locomotor rhythms. The *Drosophila melanogaster* homolog of the vertebrate circadian gene nocturnin is expressed in a subset of dorsal neurons and mediates the circadian light response. The approach should also enable the molecular dissection of many different *Drosophila* neuronal circuits.

A central goal of neurobiology is to understand animal behavior by understanding neuronal circuits. Deciphering how they function and thereby generate behavior requires identification of neuronal subtypes within a circuit, their organization and connections, as well as the contributions of individual cells to overall circuit output. Circadian rhythms in *Drosophila* and the underlying brain neuronal circuit provide an excellent substrate to achieve this end. Adult *Drosophila* locomotor activity peaks twice a day in anticipation of dawn and dusk transitions, and approximately 150 clock-containing brain neurons comprise the circuit controlling this circadian behavior. These clock neurons are divided into seven classes on the basis of their anatomical locations and characteristics. There are three groups of dorsal neurons (DN1, DN2 and DN3), lateral posterior neurons (LPN) and three groups of lateral neurons: small ventral lateral neurons (s-LNv), large ventral lateral neurons (l-LNv)

Correspondence should be addressed to M.R. (rosbash@brandeis.edu).
[4]Present addresses: Institute of Cell Biology, University of Bern, Bern, Switzerland (E.N.) and Department of Neurobiology and Physiology, Northwestern University, Evanston, Illinois, USA (E.K.).

Accession codes. GEO: Microarray data have been deposited with accession code GSE17803.

Note: Supplementary information is available on the Nature Neuroscience website.

AUTHOR CONTRIBUTIONS

E.N. and M.R. conceived the idea of this project and wrote the manuscript; E.N. conducted molecular and behavioral experiments; K.S. conducted the microarray data analysis; E.K. performed the expression profiling of the adult neurons; K.S. and S.N. contributed to the development of the protocol for the *Drosophila* cell type–specific expression profiling; E.O. and T.T. generated a NOC-RD specific antibody.

and dorsal lateral neurons (LNd). All the l-LNvs and four out of five s-LNvs express the pigment-dispersing factor (PDF) neuropeptide. Larvae have a less complex yet still functional circadian circuit[1]. Only three groups of circadian neurons, larval-LNv (lv-LNv), DN1 and DN2, are organized to effect larval circadian behaviors such as photoavoidance rhythms[2].

Recent studies have shown that adult s-LNvs (morning oscillator, M-cells) control morning activity and are essential for sustaining free-running rhythms in constant darkness, whereas a different group of cells, perhaps LNds and an s-LNv that does not express PDF (PDF-negative s-LNv, also known as 5th s-LNv), controls evening activity bouts and is thus defined as evening oscillator (E-cells)[3,4]. Although this 'M and E oscillator model' seems to explain the basic principle of the circuit organization, the roles of many other clock neurons remain undefined. Moreover, the molecules that underlie the functional diversity of clock neurons and how they interact to form functional circuits remain largely unknown.

From a molecular standpoint, circadian rhythms are generated by cell-autonomous molecular clocks present within many cells and tissues. In *Drosophila*, the core feedback loop consists of the transcriptional activator CLOCK (CLK) and its partner CYCLE (CYC), which form a heterodimer and activate the transcription of *period* and *timeless*. The *period* (PER) and *timeless* (TIM) proteins then dimerize and inhibit their own transcription by inactivating the CLK/CYC complex. There is a subsidiary loop involving the transcription factor VRILLE (VRI), which regulates *Clock* expression and thereby reinforces oscillations[5]. Many of these clock gene mRNAs manifest circadian oscillations in abundance. Post-transcriptional modifications such as phosphorylation are also critical for rhythms and regulate the stability and activity of clock transcription factors. The combination of transcriptional and post-transcriptional regulation ensures 24-h rhythmicity of the core clock. The core clock then regulates other molecules, which accumulate rhythmically or have rhythmic activity, to more directly generate overt rhythms of physiology or behavior[6].

Many of these core clock or clock output molecules may not be amenable to identification by forward genetic approaches, because of gene redundancy or additional essential functions during development. For these reasons, many researchers have turned to microarray analysis of RNA from whole fly heads collected at different circadian times to identify more candidate genes involved in the core clock or in circadian output. These studies have collectively identified many (100–200) rhythmically expressed (cycling) mRNAs in *Drosophila* heads[7–12].

However, surprisingly few new circadian-related genes have been discovered using the cycling gene expression in heads. One reason is that functionally important genes do not necessarily show cyclical RNA accumulation, as is the case in the *cycle* and *doubletime* genes[13–15]. The other possibility is that mRNA cycling in only a small number of clock neurons is masked by noncycling mRNA in other neurons and head tissues, which makes cycling undetectable by microarray analysis. Furthermore, mRNAs that are only expressed in the clock circuit or a subset should be only a tiny fraction of head RNA and may therefore escape detection in both cycling and noncycling analysis of the head RNA.

To further an understanding of circadian circuits and to circumvent mRNA oscillations as a defining property, we developed a method to identify mRNAs enriched within different subsets of well-defined types of brain neuron. Comparing the gene expression profiles from different circadian cell groups, we identified many new genes specifically expressed in all clock neurons or in important subclasses of clock neurons. We also characterized two of these new circadian genes, expressed specifically in subsets of clock cells and affecting

different aspects of rhythms. The previously uncharacterized transcription factor *Fer2* is expressed in LNvs, and it seems to be required for the specification of LNvs and LNds and therefore their ability to drive locomotor activity rhythms. The *Drosophila* homolog of the vertebrate deadenylase gene nocturnin (*nocturnin*, also known as *dnocturnin*) is expressed in only a subclass of the circadian circuit and has a role in the regulation of the circadian light response. In vertebrates, nocturnin had been identified as a cycling mRNA but has never been associated with a circadian phenotype. The methodology to profile gene expression from small numbers of different brain neurons from the circadian circuit provides a powerful approach to dissecting rhythm circuitry and should be readily applicable to characterizing other *Drosophila* brain circuits.

RESULTS

Gene expression profiling of *Drosophila* clock neurons

To profile gene expression of specific neurons within the *Drosophila* circadian circuit, we adapted a method from previous gene expression analyses of mouse brain neurons[16,17]. Briefly, targeted gene expression by the GAL4/UAS binary system and selective GAL80 expression was used to fluorescently label specific cell types with green fluorescent protein (GFP) or yellow fluorescent protein (YFP). Dissected brains were dissociated by mild protease treatment, and GFP- or YFP-expressing single cells were collected manually. Total RNA was isolated from approximately 100 cells, and poly(A) RNA was amplified and hybridized to an Affymetrix *Drosophila* genome expression array (Fig. 1a). We profiled generic, mixed neurons as well as the different sets of clock neurons, so as to identify mRNAs enriched in clock cells and eliminate general neuronal mRNAs. We then used these ‘gene expression signatures’ for the different clock cells for further molecular characterization.

In total, we purified and characterized seven different cell types. Four were from the larval brain: (i) *tim-GAL4*–positive cells (lv-tim cells), which include all clock cells (DN1s, DN2s, lv-LNvs and DN3 precursors) and two extra cells outside of the circadian circuit; (ii) lv-LNvs, labeled by *Pdf-GAL4*; (iii) cells labeled by *tim-GAL4* and *Pdf-GAL80* (lv-tim^{+}pdf^{-} cells), which include all clock cells except lv- LNvs; and (iv) pan-neuronal cells, labeled by *elav-GAL4* (lv-elav cells). The three from the adult brain were (i) *Pdf-GAL4* positive s-LNvs, (ii) *Pdf-GAL4* positive l-LNvs and (iii) pan-neuronal cells (ad-elav cells) (Fig. 1b). We also profiled the manually dissected compound eye, which includes clock-containing photoreceptor cells.

There are seven diverse groups of adult clock neurons, and only two (s-LNvs and l-LNvs) can be specifically labeled with a single driver (*Pdf-GAL4*). In contrast, the larval circadian circuit is less complex, so its clock cell subtypes can be labeled more completely with available drivers (Fig. 1b). The use of both larval and adult clock cells therefore allowed a more comprehensive genetic dissection of the circadian circuit. It also avoided identifying genes that are restricted to larval or adult clocks. All collections were done at ZT12 (zeitgeber time 12, the time of lights-off under a 12-h light:12-h dark cycle) because several known cycling clock genes are highly expressed at that time and therefore served as markers for initial validation. To provide an additional measure of mRNA enrichment, we included previously reported expression data sets from whole head samples[18] in the analysis.

To identify mRNAs enriched in all clock neurons, expression data sets from lv-tim cells, lv-LNvs and adult s- and l-LNvs were clustered as ‘clock cells’ and compared to the larval and adult elav cells (Fig. 1c). We found 84 mRNAs enriched more than twofold in clock cells relative to pan-neuronal cells (Supplementary Table 1). mRNAs of all known clock genes except *cycle* were within the top 36 clock cell–enriched mRNAs (Fig. 1c). Seventeen other

mRNAs (blue probe set names without arrows) were as enriched as the seven known clock gene mRNAs and also enriched in all the other clock cell types—namely, lv-tim$^+$pdf$^-$ cells and the eye (Fig. 1c, right panel). These 17 mRNAs are therefore prime candidates for transcripts of newly identified circadian genes highly expressed in pan-clock neurons. Other mRNAs (black probe set names) were not highly expressed in lv-tim$^+$pdf$^-$ cells (Fig. 1c, right panel), suggesting that these are more specifically enriched in LNvs and involved in specific functions of these cells. This class of mRNAs includes *Pdf*, *Hr51*, *Ir*, CG13054, *Fer2* and CG31475, which were also identified among the top 20 LNv-enriched RNAs from a separate analysis (see below).

To identify mRNAs enriched in LNvs compared to other clock neurons as well as to generic neurons, we clustered microarray data sets from larval (lv) and adult (ad) LNvs. The average expression of each mRNA in this 'LNv cluster' was compared with the average expression in the 'PDF-negative cluster'—that is, lv-tim$^+$pdf$^-$, lv-elav and ad-elav cells—and differentially expressed mRNAs were ordered by fold-difference (Fig. 2a). Sixty-three mRNAs were preferentially enriched in LNvs (fold change >2) (Supplementary Table 2).

As expected from its specificity and high abundance, *Pdf* is the top-ranked gene and is present in LNvs and in the head. Four more clock genes (*cry*, *tim*, *per* and *vri*) are ranked in the top 20, presumably because their expression is somewhat higher in LNvs than in tim$^+$pdf$^-$ cells. Highly ranked mRNAs that are not expressed in the eye and the head (Fig. 2a, blue mRNA names) are bona fide LNv-enriched mRNAs and may therefore be involved in LNv-specific functions.

Non-PDF clock neurons have been shown to be important in light-dark (LD) or constant-light (LL) conditions[19,20]. Nonetheless, these neurons are uncharacterized from a molecular standpoint. To identify mRNAs preferentially enriched in these cells relative to LNvs, we compared transcriptome data sets for the lv-tim$^+$pdf$^-$ cells with LNvs and the pan-neuronal population. Three hundred forty-two different mRNAs were enriched more than twofold in lv-tim$^+$pdf$^-$ cells (Supplementary Table 3; Fig. 2b). Because only larval cells were collected for this group, genes that are not expressed in adult clock neurons may be in this category. Genes that are also expressed in adult heads modestly are likely to be expressed in postlarval stages and probably also contribute to adult tim$^+$pdf$^-$ cell functions.

We next classified the mRNAs enriched in each subclass on the basis of gene ontology annotations (see Online Methods) and searched for functional categories that were over-represented. Notably, genes with nucleic acid binding and transcription regulator activities represented the largest population of the pan-clock neuron–enriched mRNAs. mRNAs involved in signal transduction (signal transducer) were enriched in all three cell types, suggesting the relevance of this function to the circadian circuit. However, there were marked differences in categories of mRNAs differentially expressed within the circadian circuit. mRNAs with transcription-related function were also over-represented in LNv-enriched mRNAs, whereas most of the tim$^+$pdf$^-$ cell–enriched mRNAs have various catalytic activities, including oxidoreductase, hydrolase and transferase activities (Fig. 3).

To determine whether any of these genes play a role in circadian rhythms, we tested 12 genes with available mutants, P-element insertions and UAS-RNAi lines for their effects on locomotor activity rhythms (Supplementary Table 4). The characterization of two genes specifically expressed in subgroups of clock neurons, one in LNvs and a second in tim$^+$pdf$^-$ cells, is described below. A third gene, expressed in all clock neurons, will be presented elsewhere.

Fer2 is required for lateral neuron function

Fer2 (*48-related 2*) was identified as one of the most enriched mRNAs in both larval and adult PDF-positive neurons. *Fer2* encodes a basic helix-loop-helix protein closely related to mammalian *p48*, also known as *PTF1*, a transcription factor specific to pancreatic exocrine cells and brain neurons[21–23]. The biological function of *Fer2* has not, to our knowledge, been studied yet.

We assayed the locomotor behavior of the *PBac{RB}Fer2* strain, which has a P element approximately 100 nucleotides upstream of the first ATG of *Fer2* (Fig. 4a). *Fer2* mRNA abundance in homozygous *PBac{RB}Fer2* flies was only 2% of that in wild type (Fig. 4b). Among homozygous *PBac{RB}Fer2* flies, 100% showed no rhythmic behavior in constant-dark (DD) conditions and were entirely arrhythmic even in LD; two different strains hemizygous for the *PBac{RB}Fer2* gene (P element in one homologous chromosome and a deletion in the other) were similarly arrhythmic (Fig. 4c). In contrast, heterozygous mutants had normal behavior under both conditions.

Coimmunostaining of homozygous *PBac{RB}Fer2* fly brains with anti-PER and anti-PDF at different time points showed that *Fer2* mutants did not express detectable amounts of PDF in LNvs. Notably, PER staining was absent in LNds as well as LNvs. In contrast, PER staining as well as cycling appeared normal in dorsal clock neurons, at least under LD conditions (Fig. 5a,b). Results were similar in the hemizygous *PBac{RB}Fer2* flies (data not shown). PDF and PER was also undetectable in the LNvs of the *Fer2* mutant third-instar larval brain (Supplementary Fig. 1). As several lines of evidence suggest that LNvs (M-cells) are required for rhythms in DD, and E-cells (including LNds) are critical for rhythms in LD[3,4], the absence of detectable PER in both groups explains the behavioral arrhythmicity of the *Fer2* mutant flies.

This absence of PER and PDF expression can be explained in several ways, including the absence of lateral neurons from the *Fer2* mutant strains. To assess this possibility, we stained wild-type and mutant brains with antibodies to CLK. The staining showed that the *Fer2* mutant strain had significantly fewer LNvs and LNds than control flies ($P < 0.001$, two-sample *t*-test). Even when evident, CLK staining was noticeably weaker in the mutant lateral neurons than in control lateral neurons. Notably, not a single brain expressed detectable PDF even when CLK expression was visible in the lateral neuron region. In contrast, the number and staining intensity of CLK-positive dorsal neurons was indistinguishable between mutant and control brains (Fig. 5c,d). Notably, *cry-GAL4* expression was also undetectable in the *Fer2* mutant LNvs and was very weak in the *Fer2* mutant LNds (Supplementary Fig. 2a,b). Although this unusual CLK and *cry* expression does not rule out the possibility that lateral neuron numbers are normal and that these genes are very poorly expressed in those cells, the LNv gene expression program is, at a minimum, severely impaired in the *Fer2* mutant. As *Fer2* is expressed throughout development, it is likely to be pivotal in the development and/or maintenance of LNvs and LNds.

nocturnin regulates light-mediated behavioral entrainment

nocturnin was among the top 20 mRNAs by enrichment in $tim^{+}pdf^{-}$ cells. It is a homolog of *Saccharomyces cerevisiae CCR4*, a dead-enylase involved in mRNA decay. Vertebrate homologs of *nocturnin* (*Xenopus laevis* and mammalian) are rhythmically expressed under the control of the circadian clock in a variety of tissues, such as *Xenopus* retina and several mouse tissues[24,25]. A recent study on mouse nocturnin demonstrated that it regulates lipid metabolism, probably through the post-transcriptional regulation (deadenylation) of target mRNAs[26,27]. In contrast, *Drosophila nocturnin* is uncharacterized.

There are three reported *Drosophila nocturnin* transcripts, *RC*, *RD* and *RE* (Fig. 6a). We assayed the expression of each isoform in adult heads by real-time PCR and found *nocturnin-RD* RNA to accumulate rhythmically, with a peak around ZT8 (Fig. 6b). Like its RNA, NOCTURNIN-RD (NOC-RD) protein accumulates rhythmically; it peaks at around ZT12, somewhat later than the *RD* RNA, as judged by western blotting using a NOC-RD–specific monoclonal antibody (Fig. 6c). Cycling of NOC-RD immunoreactivity was observed only in a subgroup of clock neurons, the DN3s (verified by tim-GAL4 colocalization (Supplementary Fig. 3). A group of cells within the pars intercerebralis were nonspecifically labeled by the antibody to NOC-RD (tested by RNAi, data not shown; Fig. 6d).

To investigate the possible function of *nocturnin*, we used an RNAi strategy to knock down *nocturnin* gene expression in clock cells. *UAS-RNAi-1* specifically targets the RD isoform, whereas *UAS-RNAi-2* targets all three isoforms (Fig. 6a). *tim-GAL4, UAS-RNAi-1* decreased *RD* RNA to approximately 35% of wild-type (that is, *tim-GAL4*) abundance, whereas the other two isoforms were not greatly affected. *tim-GAL4, UAS-RNAi-2* decreased the *RE* and *RC* isoforms to ~20% of control values, whereas the *RD* isoform was reduced only to ~60% of the control (Fig. 6e). This may be due to differences in RNA secondary structures between the different mRNA isoforms, or it could be due to the regulation of the *RD* isoform stability by RE or RC.

Both *nocturnin*-knockdown lines showed essentially wild-type free-running rhythms in DD (Fig. 6f). Notably, most of the RD-knockdown flies (*tim-GAL4, UAS-RNAi-1*) were rhythmic under constant light. Wild-type flies are arrhythmic in LL[28]. About 50% of the rhythmic flies showed complex activity patterns (Fig. 7a,b). In contrast, RE- and RC-knockdown (*tim-GAL4, UAS-RNAi-2*) had no impact on LL behavior. Because the *RD* isoform is specifically expressed in a subset of DN3s but not in LNvs, the LL-rhythmic phenotype is most likely caused by the reduced *nocturnin-RD* in DN3s. Consistent with this notion, *pdf-GAL4, UAS-RNAi-1* flies were arrhythmic in LL, like wild type. Independent insertion lines of *UAS-RNAi-1* (NIG, 31299 R-6) and *UAS-RNAi-2* (VDRC, 45421) gave similar results (data not shown).

Immunostaining with anti-PER showed PER cycling in DN1s and as well as in DN3s, DN2s and the LPNs in the RD-knockdown flies in LL (Fig. 7c,d). The result that dorsal neurons showed sustained molecular rhythms in LL-rhythmic flies is consistent with previous studies in which overexpression of *period*, *shaggy* or *morgue* in clock neurons causes LL rhythmicity[19,20]. This suggests that the *nocturnin-RD* knockdown in DN3s triggers a cellular response similar to that in previous overexpression manipulations that result in LL phenotypes.

To learn more about light-response behavior in *nocturnin-RD* knockdown flies, we examined a light-mediated phase response curve (PRC). The *nocturnin-RD* knockdown flies showed a shorter phase delay in the early night compared to wild-type flies (Fig. 7e). All of the *nocturnin-RD* results therefore indicate that this gene contributes to the light-mediated behavioral response (Supplementary Fig. 4, and see Discussion).

DISCUSSION

We applied a new method of profiling gene expression from specific cells of the *Drosophila* larval and adult brain to the neuronal circuit controlling circadian rhythms. The approach identified mRNAs highly enriched in all clock neurons, as well as mRNAs enriched in two subgroups of clock cells: PDF-positive LNvs and $tim^{+}pdf^{-}$ cells. The three sets of mRNAs were more different than expected. From among the mRNAs identified, we characterized

two new circadian genes. *Fer2* was enriched in LNvs and is pivotal in the specification of a subset of clock neurons. *nocturnin* was enriched in $tim^{+}pdf^{-}$ cells and contributes to light-mediated circadian behaviors. To our knowledge, this study is the first to attempt a dissection of a defined neuronal circuit on the basis of cell type–specific gene expression profiling.

Other approaches exist for cell-specific profiling of gene expression. These include FACS-based techniques and laser capture microdissection, as well as a combination of FACS and differential tagging—for example, tagged poly(A)-binding protein or tagged ribosomal proteins for polyribosome purification[29–33]. However, some of these methods may have an inadequate signal-to-noise ratio when starting with a very small number of tagged cells and whole brain extracts. In contrast, manual sorting allows mRNA analysis from very small numbers of cells. It also seems harmless to RNA and is therefore ideal for neuronal circuits comprising multiple cell types, each with a small number of cells.

All known circadian genes except *cycle* were ranked in the top 40 generic clock cell–enriched mRNAs (Fig. 1c). Such analyses have not been performed in mammals, to our knowledge; that is, it is not known to what extent clock gene mRNAs are enriched in suprachiasmatic nucleus clock neurons.

Given that a typical cell expresses many thousands of genes, the clock neurons show a remarkable enrichment of genes involved in a single biological pathway. The probability of selecting 10 probe sets for clock genes in the randomly chosen 40 probe sets out of the entire 13,693 probe sets is $P = 1.12 \times 10^{-17}$ (calculated from the hypergeometric distribution). This further suggests that it is statistically probable that other circadian genes are also in the highly enriched list. Indeed, we found that *Thor* (*Drosophila 4E-BP*), a gene highly enriched in all clock cells, contributes to circadian function (unpublished data). Taken together with the 2 other genes described here, at least 3 out of 12 genes examined (25%) have roles in the circadian clock. For reasons such as redundancy or strong effects only under certain conditions, this must underestimate the frequency of circadian mRNAs. We therefore predict that many more genes identified in this study will play a role in rhythms and lead to further understanding of relevant processes, core timekeeping, and the neuronal network through which behavioral rhythms is orchestrated.

It is notable that mRNA oscillations were not necessary to identify circadian genes. Remarkably, *cry* and *Clk* mRNAs, cycling clock genes with a trough around ZT12, were also found in the short list of the clock cell–enriched mRNAs (Fig. 1c). Moreover, *Fer2* as well as *Thor* mRNAs show no evidence of cycling (data not shown). Finally, there is little overlap between the clock cell–enriched mRNAs identified here and the cycling mRNAs from whole heads reported in previous studies[7–12], except for the known cycling clock genes.

Many of the pan-clock cell–enriched and LNv-enriched mRNAs are identified as having transcriptional regulator or DNA binding activity (Fig. 3). This underscores the importance of the transcription feedback loop and transcriptional regulation more generally in the core timekeeping mechanism, as well as in clock output. In contrast, most of the gene expression differentially enriched in $tim^{+}pdf^{-}$ cells have catalytic activity, including oxidoreductase, hydrolase and transferase activity. This difference with LNv mRNAs likely reflects different contributions of LNvs and $tim^{+}pdf^{-}$ cells to the circadian circuit. The former are the main pacemaker cells (M-cells) and drive locomotor rhythms; perhaps many of these transcription-relevant genes contribute to the core clock or its output through transcriptional mechanisms. The latter include the dorsal neurons, which are known to be involved in the light input as well as in a behavioral output pathway[19,20] (C.H. Tang, E. Hinteregger, Y.

Shang and M. Rosbash, unpublished data). Redox regulation of signaling proteins (including kinases, phosphatases, small GTPases, guanylate cyclases and adaptor proteins) has been shown to modulate their function[34]. Notably, previous studies have indicated a role for redox in light-dependent CRYPTOCHROME (CRY) degradation, which is known to be involved in phase resetting of the clock[35,36]. It is therefore plausible that some dorsal neuron–enriched oxidoreductases play roles in light-input signaling within the dorsal neurons. We anticipate more generally that the newly identified genes specifically expressed in $tim^{+}pdf^{-}$ cells will help define additional dorsal neuron functions and their underlying mechanisms.

The basic helix-loop-helix protein FER2 was identified as LNv-enriched. The *Fer2* mutation severely impairs clock gene expression in LNds as well as adult and larval LNvs. This includes expression of the key circadian transcription factor *Clk*, which appears weak and/or absent only from the lateral neuron region of the fly brain (Fig. 5c). Notably, the *Fer2* mutant phenotype is much stronger than that of the strongest known *Clk* mutant: although *Clk* mutation abolishes PDF expression in adult s-LNvs, l-LNvs are normal in Clk^{jrk} (ref. 13). A parsimonious interpretation is therefore that *Fer2* is predominantly upstream of *Clk*, *cry* and PDF expression in lateral neurons. As the LNds have evening oscillator (E-cell) activity[37,38] and the s-LNvs are morning oscillator cells (M-cells), *Fer2* may function as a master transcriptional regulator for the development and/or maintenance of the circadian circuit subset with oscillator activity.

FER2 probably exerts its function cell autonomously, as *in situ* hybridization with an antisense *Fer2* probe revealed expression in the lateral protocerebrum, where LNvs as well as LNds are located (data not shown). Coregulation of M- and E-cells is consistent with recent work on interspecific regulation of *Pdf* expression[39], which also suggests that there are additional transcription factors that underlie the differences between these important pacemaker cells. This makes the common and cell type–specific targets of FER2 of particular interest.

nocturnin is enriched in $tim^{+}pdf^{-}$ cells, and the cycling isoform, *nocturnin-RD*, is specifically expressed in a subset of DN3s. There is as yet no evidence that the noncycling isoforms contribute to circadian rhythms. Indeed, a very recent study on *curled* (shown to encode NOC) suggests that it has noncircadian functions[40]. We therefore consider it unlikely that the NOC-RD knockdown phenotype is due to an altered balance of noncycling and cycling isoforms, and the simplest interpretation is that the NOC-RD isoform has a dedicated circadian role. Consistent with published studies[19,20], this LL rhythmic phenotype is associated with molecular rhythms in the dorsal neurons. Although it is possible that the NOC-RD protein accumulation pattern is more complex than a simple circadian variation (see Fig. 6c), the peaking of NOC-RD protein abundance at about lights-off suggests that *nocturnin-RD* is involved in processing the light signal in the early night. Indeed, the knockdown of *nocturnin-RD* reduced the early night light pulse-mediated phase delay (Fig. 7e). Notably, vertebrate *nocturnin* was identified as cycling mRNA in *Xenopus* eyes but has never been associated with a circadian phenotype. The results here indicate that *nocturnin* is indeed a circadian gene and may have an ancient and conserved association with photoreception.

Light is received by several pathways, including photoreceptor organs and the intracellular photoreceptor CRY, and processed through as-yet unknown neuronal mechanisms to modulate behavior rhythms. CRY in PDF-negative clock cells plays a major role in light-mediated phase shift in the early night and the entrainment of the evening activity peak[41]. Subsets of DN1s express CRY and receive light directly, whereas most if not all DN3s do not[42]. The fact that the NOC-RD knockdown phenocopies the overexpression of *shaggy*,

which stabilizes the TIM/CRY complex and inhibits circadian light responses, suggests that NOC-RD interacts with CRY-mediated light processing. We therefore suggest that *nocturnin-RD* functions between DN3s and CRY-expressing DN1s to process light-input information in the early night. It may also be involved in signaling light information to other clock neurons, including DN2s. Light information is ultimately communicated to the central pacemaker M-cells (Supplementary Fig. 4).

The sequence conservation of *nocturnin* with the yeast deadenylase *CCR4* and vertebrate homologs suggests that NOC-RD regulates the stability or translatability of mRNAs involved in mediating a light response and perhaps neuronal signaling. These would be novel connections between these neuronal functions and post-transcriptional regulation. Identification of target mRNAs of NOC-RD is therefore an important challenge for future studies.

The gene expression profiles of the three sets of circadian neurons are sufficiently different that a substantial number of mRNAs probably underlie the different roles of these circadian circuit components. The *Fer2 and nocturnin* genes validate the profiling and begin to provide insight into some of these distinct functions. These genes and others identified in this study should also lead to new GAL4 drivers, which will be able to label and manipulate additional elements of the circuit. For example, the promoter of *nocturnin* might lead the isolation of *RD*-expressing DN3s, which might form a functionally distinct subset within this numerous (~40 cells per hemisphere) neuronal group. These strategies should be applicable to the dissection of any *Drosophila* neuronal circuit for which well-characterized fluorescent protein expression patterns can be generated.

ONLINE METHODS

Gene expression analysis of the manually sorted cells from *Drosophila* brains

The cell sorting, RNA isolation and preparation protocol was modified from the method described previously[16,17]. Vials containing young adult flies and larva were entrained in 12 h light:12 h dark (LD) for at least 3 d and collected at ZT12. Vials were immediately transferred onto ice and kept on ice during the dissection. We dissected brains from early third instar larvae and young adults into ice-cold modified dissecting saline (9.9 mM HEPES-KOH buffer, 137 mM NaCl, 5.4 mM KCl, 0.17 mM NaH_2PO_4, 0.22 mM KH_2PO_4, 3.3 mM glucose, 43.8 mM sucrose, pH 7.4)[43] containing 50 μM D(−)-2-amino-5-phosphonovaleric acid (AP5), 20 μM 6,7-dinitroquinoxaline-2,3-dione (DNQX), 0.1 μM tetrodotoxin (TTX), and immediately transferred them into modified SM^{active} medium (SM^{active} medium containing 5 mM Bis-Tris, 50 μM AP5, 20 μM DNQX, 0.1 μM TTX) on ice[44]. Approximately 50 brains were collected within 1 h of the start of the dissections. For sorting cells from lv-tim cells and lv-tim^+pdf^- cells, we carefully removed the ring gland and ventral ganglion and used only the central brains. For sorting lv-LNvs, we removed ventral ganglia from the rest of the brains. Brains were digested with L-cysteine-activated papain (50 units ml^{-1} in dissecting saline; Worthington) for 10 min (larval brains) or 20 min (adult brains) at 25 °C. Digestion was quenched with a fivefold volume of the medium, and brains were washed twice with the chilled medium. Brains were triturated with a flame-rounded 1,000-μl pipetter tip with filter followed by a flame-rounded 200-μl pipetter tip with filter until most of the tissues were dissociated to single cells. The resulting cell suspension was diluted in the chilled medium and transferred to two 60-mm Petri dishes with Sylgard (Dow Corning) substratum. Under a fluorescence-dissecting microscope, we manually sorted GFP- or YFP-positive cells from one dish at a time, while keeping the other dish on ice. We transferred collected cells to the second dish, which was kept on ice, then reselected GFP- or YFP-positive cells and transferred them to a third dish, and we further selected only GFP- or YFP-positive cells and transferred them to a tube for RNA extraction. After three

rounds of sorting, approximately 100 fluorescent cells were pooled for each microarray experiment. Total RNA from collected cells was extracted and poly(A) RNA was amplified by two-cycle linear amplification, processed as previously described[17] and hybridized to a GeneChip *Drosophila* Genome 2.0 array (Affymetrix). Two or three biological replicates were profiled for each cell type. Adult eye samples were prepared from manually dissected compound eyes.

Microarray data analysis. Scanned Affymetrix image data were processed with the Affymetrix GCOS software to convert to probe level signals. The probe signal files were then processed with the gcrma package (Bioconductor) to normalize and calculate summary values for each probe set using the GCRMA algorithm (http://www.bioconductor.org/packages/2.0/bioc/html/gcrma.html).The rest of the analysis was performed using in-house software written in Python (http://www.python.org/) and R (http://www.r-project.org/). Affymetrix annotation (Drosophila 2 annotations, CSV format) was used to associate probe sets and genes. When the average of the summary values of replicates across all the samples was ≤5.5, the probe set was filtered out as low or unexpressed.

For Figure 1c, lv-tim cells, lv-LNvs, s-LNvs and l-LNvs were compared to lv-elav cells and ad-elav cells. A *t*-test threshold of $P < 0.001$ and fold change > 8 yielded 84 probe sets. For Figure 2a, lv-LNvs, s-LNvs and l-LNvs were compared to lv-tim^{+}pdf^{-} cells, lv-elav cells and ad-elav cells. A *t*-test threshold of $P < 0.0001$ and fold change > 8 yielded 63 probe sets. For Figure 2b, lv-tim^{+}pdf^{-} cells were compared to lv-LNvs, s-LNvs, l-LNvs, lv-elav cells and ad-elav cells. A *t*-test threshold of $P < 0.0001$ and fold change > 8 yielded 342 probe sets. False discovery rates for those selections were calculated by dividing an estimate of the number of false positives by the actual number of selected genes. The number of false positives was estimated by 100 trials consisting of random shuffling of the samples followed by the same filtering procedure applied to the actual case (filtering by *t*-test *P*-value and fold change)[45].

Enrichment *P*-values of clock genes in Figure 1c were calculated using a hypergeometric distribution. We obtained a total of 7 clock genes out of 8 (*tim, per, Clk, cyc, cwo, Pdp1, cry, vri*) in the list of 39 probe sets (after removing *tim* probe set duplication from the 40 top-ranked probe sets shown in Fig. 1c) from a total of 12,768 unique probe sets (unique in terms of gene symbol defined by the Affymetrix annotation).

Gene ontology data were downloaded from http://www.geneontology.org/, version 14:04:2008 19:30. The Affymetrix annotation was used to associate probe sets and gene ontology terms. For a given list of probe sets, it was first reduced to a list with unique symbols; then over-representation probabilities of gene ontology terms were calculated by hypergeometric distribution using an in-house Python program. Because not all the genes had gene ontology annotations, we calculated the percentage of the genes with the given annotation among all annotated genes (Fig. 3). There were 63 gene ontology–annotated genes (out of 84) in the clock cell–enriched gene category, 44 genes (out of 63) in LNv-enriched genes, and 200 genes (out of 342) in tim^{+}pdf^{-} cell–enriched genes.

Fly strains

All GAL4 lines used in this study have been described previously: *tim-GAL4* (ref. 46), *Pdf-GAL4* (ref. 4), *Pdf-GAL80* (ref. 4) and *cry(39)-GAL4* (ref. 47). Lines used to label cell types for cell sorting were as follows: *y w*; *tim-GAL4, UAS-2xEYFP/CyO*, which were generated by recombining *y w*; *tim-GAL4/CYO* and *y w*; *P{w[+mC]=UAS-2xEYFP}AH2* (Bloomington Stock Center) and used to sort *tim-GAL4* labeled cells. lv-tim^{+}pdf^{-} cells were collected from *y w*; *tim-GAL4, UAS-2xEYFP/CyO; Pdf-GAL80*. *Pdf-GAL4*–positive cells were sorted from *y w*, *UAS-mCD8*::*GFP; Pdf-GAL4*. Larval elav cells were labeled by

crossing *UAS-EGFP* and *w*;; *elav-GAL4*. Adult elav cells were labeled by crossing *UAS-EGFP* males and virgin females of the *C155-GAL4* enhancer trap line, and F_1 males and females were used. *tim-GAL4* in adult brains is expressed in many glia and therefore was not used to label adult cells for cell sorting.

The following lines were also obtained from Bloomington Stock Center: w^{1118}; *PBac{RB}Fer2*^{e03248}, w^{1118}; *Df(3R)sbd104/TM6B* (referred to herein as *Df1*) w^{1118}; *Df(3R)sbd45/TM6B* (referred to as *Df2*). Genotypes of flies used in the behavior assay of *Fer2* mutants (Fig. 4c) were as follows: *PBac{RB}Fer2/+*, w^{1118}; *PBac{RB}Fer2*^{e03248}*/TM6B. PBac{RB}Fer2*, w^{1118}; *PBac{RB}Fer2*^{e03248}*. Df1/+*, w^{1118}; *Df(3R)sbd104/TM6B. Df1/PBac{RB}Fer2*, w^{1118}; *Df(3R)sbd104/PBac{RB}Fer2*^{e03248}*. Df2/+*, w^{1118}; *Df(3R)sbd45/TM6B. Df2/PBac{RB}Fer2*, w^{1118}; *Df(3R)sbd45/PBac{RB}Fer2*^{e03248}.

The RNAi line against *nocturnin*, *UAS-RNAi-1* (31299-R1) was obtained from the National Institute of Genetics (Sizuoka, Japan), and *UAS-RNAi-2* (45442) from the Vienna *Drosophila* RNAi Center. Genotypes of flies used to study behavior of *nocturnin*-knockdown flies (Figs. 6 and 7) were as follows: *tim-GAL4, y w*; *tim-GAL4/+*. *UAS-RNAi-1*, *y w*; *UAS-RNAi-1/+*. *tim>RNAi-1*, *y w*; *tim-GAL4/+*. *UAS-RNAi-1/+*, *UAS-RNAi-2*, *y w*; *UAS-RNAi-2/+*. *tim>RNAi-2, y w; tim-GAL4/+;UAS-RNAi-2/+*. *pdf-GAL4, y w; Pdf-GAL4/+*. *pdf>UAS-RNAi-1*, *y w*; *Pdf-GAL4/+*;*UAS-RNAi-1/+*.

Behavior assays

LD, DD and LL locomotor behavior assays and PRC experiments were performed as described previously[20].

Production of antibody to NOC TURNIN-RD

We generated a rat monoclonal antibody that specifically recognized NOC-RD using the rat lymph node method[48]. A WKY/Crj rat was immunized with synthetic peptide (ELLEDDDKPPQLFS)-conjugated keyhole limpet hemocyanin. After 3 weeks, rat lymphocytes were fused with mouse myeloma Sp2 cells. We screened the NOC-RD–specific antibody by ELISA and immunostaining using hybridoma supernatants and selected clone 2C4.

Immunostaining

Immunostaining of *Drosophila* brains using anti-PER and anti-PDF was performed as described previously[49]. CLK immunostaining was performed with guinea pig antiserum to CLK (GP50), a gift from P. Hardin, as described[50]. For immunostaining for NOC-RD, heads were fixed in 2% paraformaldehyde in PBST (PBS, 0.5% Triton X-100 (Sigma)) on ice for 45 min, and washed twice with PBST, incubated with blocking solution (10% goat serum, PBST) for 1 h at 25 °C, then incubated with anti-NOC-RD (2C4) (25 μg ml^{-1}) for two overnights at 4 °C. Alexa Fluor 488 goat anti–rat immunoglobulin G (Invitrogen) was used as a secondary antibody.

RNA analysis by real-time PCR

Total RNA was prepared from embryos or adult heads with Trizol (Invitrogen). RNA (1.5 to 3 μg) was reverse-transcribed with oligo$(dT)_{12–18}$ using SuperScript III (Invitrogen) and the cDNA used as a template for quantitative real-time PCR performed with a Corbett Research Rotor-Gene 3000 real-time cycler. The PCR mixture contained Platinum Taq Polymerase (Invitrogen), an optimized concentration of Sybr green (Invitrogen), and the appropriate primers: *Fer2* forward, 5′-CAACTGCGTCCAGCTACAAA-3′; *Fer2* reverse, 5′-CTCGTACGGAAAGGTGGGTA-3′; *nocturnin-RC* forward, 5′-

CATTAAGCGAGCCAACAAGG-3′; *nocturnin-RC* reverse, 5′-ATGAACCCATTCTGGTCAGC-3′; *nocturnin-RD* forward, 5′-TGCAACTGGAATGGGAGAGT-3′; *nocturnin-RD* reverse, 5′-TCCTGGGAGTCCACATTGTT-3′; *nocturnin-RE* forward, 5′-AGGCTGCAAAATGGAAACAC-3′; *nocturnin-RE* reverse, 5′-GCTATCTTTCGGCTGCTGAC-3′; *Ef1*β forward, 5′-GTCATCGAGGACGACAAGGT-3′; *Ef1*β reverse, 5′-TCTTGTTGAAGGCAGCAATG-3′. Cycling parameters were 95 °C for 3 min, followed by 40 cycles of 95 °C for 30 s, 55 °C for 45 s and 72 °C for 45 s. Fluorescence intensities were plotted versus the number of cycles by using an algorithm provided by the manufacturer. mRNA was quantified using a calibration curve based on dilution of concentrated cDNA. mRNA values for *Fer2* and *nocturnin* were normalized to that of *elongation factor 1*β (*Ef1*β).

Supplementary Material

Refer to Web version on PubMed Central for supplementary material.

Acknowledgments

We thank P. Hardin (Texas A&M University) for antisera to CLK as well as the Bloomington Stock Center, National Institute of Genetics of Japan (NIG) and Vienna Drosophila RNAi Center (VDRC) for fly stocks. We are grateful to J. Menet, W. Luo, K. Abruzzi, S. Bradley, L. Griffith, P. Garrity, S. Waddell, R. Allada, Y. Shang, P. Emery and J. Blau for comments on the manuscript. Y. Shang also provided the protocol for culture media preparation, and N. Francis helped with brain dissections. Some of this work was supported by a fellowship to E.N. from the Charles A. King Trust.

References

1. Kaneko M, Helfrich-Forster C, Hall JC. Spatial and temporal expression of the *period* and *timeless* genes in the developing nervous system of *Drosophila*: newly identified pacemakers candidates and novel features of clock gene product cycling. J. Neurosci. 1997; 17:6745–6760. [PubMed: 9254686]
2. Mazzoni EO, Desplan C, Blau J. Circadian pacemaker neurons transmit and modulate visual information to control a rapid behavioral response. Neuron. 2005; 45:293–300. [PubMed: 15664180]
3. Grima B, Chelot E, Xia R, Rouyer F. Morning and evening peaks of activity rely on different clock neurons of the *Drosophila* brain. Nature. 2004; 431:869–873. [PubMed: 15483616]
4. Stoleru D, Peng Y, Agosto J, Rosbash M. Coupled oscillators control morning and evening locomotor behaviour of *Drosophila*. Nature. 2004; 431:862–868. [PubMed: 15483615]
5. Yu W, Hardin PE. Circadian oscillators of *Drosophila* and mammals. J. Cell Sci. 2006; 119:4793–4795. [PubMed: 17130292]
6. Gallego M, Virshup DM. Post-translational modifications regulate the ticking of the circadian clock. Nat. Rev. Mol. Cell Biol. 2007; 8:139–148. [PubMed: 17245414]
7. Ceriani MF, et al. Genome-wide expression analysis in *Drosophila* reveals genes controlling circadian behavior. J. Neurosci. 2002; 22:9305–9319. [PubMed: 12417656]
8. Claridge-Chang A, et al. Circadian regulation of gene expression systems in the *Drosophila* head. Neuron. 2001; 32:657–671. [PubMed: 11719206]
9. Keegan KP, Pradhan S, Wang JP, Allada R. Meta-analysis of *Drosophila* circadian microarray studies identifies a novel set of rhythmically expressed genes. PLoS Comput. Biol. 2007; 3:e208. [PubMed: 17983263]
10. Lin Y, et al. Influence of the period-dependent circadian clock on diurnal, circadian, and aperiodic gene expression in *Drosophila melanogaster*. Proc. Natl. Acad. Sci. USA. 2002; 99:9562–9567. [PubMed: 12089325]
11. McDonald MJ, Rosbash M. Microarray analysis and organization of circadian gene expression in *Drosophila*. Cell. 2001; 107:567–578. [PubMed: 11733057]

12. Ueda HR, et al. Genome-wide transcriptional orchestration of circadian rhythms in *Drosophila*. J. Biol. Chem. 2002; 277:14048–14052. [PubMed: 11854264]
13. Park JH, et al. Differential regulation of circadian pacemaker output by separate clock genes in *Drosophila*. Proc. Natl. Acad. Sci. USA. 2000; 97:3608–3613. [PubMed: 10725392]
14. Rutila JE, et al. CYCLE is a second bHLH-PAS clock protein essential for circadian rhythmicity and transcription of *Drosophila* period and timeless. Cell. 1998; 93:805–814. [PubMed: 9630224]
15. Kloss B, et al. The *Drosophila* clock gene double-time encodes a protein closely related to human casein kinase Iε. Cell. 1998; 94:97–107. [PubMed: 9674431]
16. Hempel CM, Sugino K, Nelson SB. A manual method for the purification of fluorescently labeled neurons from the mammalian brain. Nat. Protoc. 2007; 2:2924–2929. [PubMed: 18007629]
17. Sugino K, et al. Molecular taxonomy of major neuronal classes in the adult mouse forebrain. Nat. Neurosci. 2006; 9:99–107. [PubMed: 16369481]
18. Kadener S, Stoleru D, McDonald M, Nawathean P, Rosbash M. Clockwork Orange is a transcriptional repressor and a new *Drosophila* circadian pacemaker component. Genes Dev. 2007; 21:1675–1686. [PubMed: 17578907]
19. Murad A, Emery-Le M, Emery P. A subset of dorsal neurons modulates circadian behavior and light responses in *Drosophila*. Neuron. 2007; 53:689–701. [PubMed: 17329209]
20. Stoleru D, et al. The *Drosophila* circadian network is a seasonal timer. Cell. 2007; 129:207–219. [PubMed: 17418796]
21. Moore AW, Barbel S, Jan LY, Jan YN. A genomewide survey of basic helix-loop-helix factors in *Drosophila*. Proc. Natl. Acad. Sci. USA. 2000; 97:10436–10441. [PubMed: 10973473]
22. Krapp A, et al. The bHLH protein PTF1-p48 is essential for the formation of the exocrine and the correct spatial organization of the endocrine pancreas. Genes Dev. 1998; 12:3752–3763. [PubMed: 9851981]
23. Hoshino M, et al. Ptf1a, a bHLH transcriptional gene, defines GABAergic neuronal fates in cerebellum. Neuron. 2005; 47:201–213. [PubMed: 16039563]
24. Green CB, Besharse JC. Identification of a novel vertebrate circadian clock-regulated gene encoding the protein nocturnin. Proc. Natl. Acad. Sci. USA. 1996; 93:14884–14888. [PubMed: 8962150]
25. Wang Y, et al. Rhythmic expression of Nocturnin mRNA in multiple tissues of the mouse. BMC Dev. Biol. 2001; 1:9. [PubMed: 11394964]
26. Garbarino-Pico E, et al. Immediate early response of the circadian polyA ribonuclease nocturnin to two extracellular stimuli. RNA. 2007; 13:745–755. [PubMed: 17400819]
27. Green CB, et al. Loss of Nocturnin, a circadian deadenylase, confers resistance to hepatic steatosis and diet-induced obesity. Proc. Natl. Acad. Sci. USA. 2007; 104:9888–9893. [PubMed: 17517647]
28. Konopka RJ, Pittendrigh C, Orr D. Reciprocal behaviour associated with altered homeostasis and photosensitivity of *Drosophila* clock mutants. J. Neurogenet. 1989; 6:1–10. [PubMed: 2506319]
29. Roy PJ, Stuart JM, Lund J, Kim SK. Chromosomal clustering of muscle-expressed genes in *Caenorhabditis elegans*. Nature. 2002; 418:975–979. [PubMed: 12214599]
30. Doyle JP, et al. Application of a translational profiling approach for the comparative analysis of CNS cell types. Cell. 2008; 135:749–762. [PubMed: 19013282]
31. Heiman M, et al. A translational profiling approach for the molecular characterization of CNS cell types. Cell. 2008; 135:738–748. [PubMed: 19013281]
32. Yang Z, Edenberg HJ, Davis RL. Isolation of mRNA from specific tissues of *Drosophila* by mRNA tagging. Nucleic Acids Res. 2005; 33:e148. [PubMed: 16204451]
33. Hoopfer ED, Penton A, Watts RJ, Luo L. Genomic analysis of *Drosophila* neuronal remodeling: a role for the RNA-binding protein Boule as a negative regulator of axon pruning. J. Neurosci. 2008; 28:6092–6103. [PubMed: 18550751]
34. Finkel T. Oxygen radicals and signaling. Curr. Opin. Cell Biol. 1998; 10:248–253. [PubMed: 9561849]
35. Lin FJ, Song W, Meyer-Bernstein E, Naidoo N, Sehgal A. Photic signaling by cryptochrome in the *Drosophila* circadian system. Mol. Cell. Biol. 2001; 21:7287–7294. [PubMed: 11585911]

36. Sathyanarayanan S, et al. Identification of novel genes involved in light-dependent CRY degradation through a genome-wide RNAi screen. Genes Dev. 2008; 22:1522–1533. [PubMed: 18519643]
37. Rieger D, Shafer OT, Tomioka K, Helfrich-Forster C. Functional analysis of circadian pacemaker neurons in *Drosophila melanogaster*. J. Neurosci. 2006; 26:2531–2543. [PubMed: 16510731]
38. Picot M, Cusumano P, Klarsfeld A, Ueda R, Rouyer F. Light activates output from evening neurons and inhibits output from morning neurons in the *Drosophila* circadian clock. PLoS Biol. 2007; 5:e315. [PubMed: 18044989]
39. Bahn JH, Lee G, Park JH. Comparative analysis of Pdf-mediated circadian behaviors between *Drosophila melanogaster* and *D. virilis*. Genetics. 2009; 181:965–975. [PubMed: 19153257]
40. Gronke S, Bickmeyer I, Wunderlich R, Jackle H, Kuhnlein RP. *curled* encodes the *Drosophila* homolog of the vertebrate circadian deadenylase Nocturnin. Genetics. 2009; 183:219–232. [PubMed: 19581445]
41. Emery P, et al. *Drosophila* CRY is a deep brain circadian photoreceptor. Neuron. 2000; 26:493–504. [PubMed: 10839367]
42. Yoshii T, Todo T, Wulbeck C, Stanewsky R, Helfrich-Forster C. Cryptochrome is present in the compound eyes and a subset of *Drosophila*'s clock neurons. J. Comp. Neurol. 2008; 508:952–966. [PubMed: 18399544]
43. Jiang SA, Campusano JM, Su H, O'Dowd DK. *Drosophila* mushroom body Kenyon cells generate spontaneous calcium transients mediated by PLTX-sensitive calcium channels. J. Neurophysiol. 2005; 94:491–500. [PubMed: 15772240]
44. Kuppers-Munther B, et al. A new culturing strategy optimises *Drosophila* primary cell cultures for structural and functional analyses. Dev. Biol. 2004; 269:459–478. [PubMed: 15110713]
45. Tusher VG, Tibshirani R, Chu G. Significance analysis of microarrays applied to the ionizing radiation response. Proc. Natl. Acad. Sci. USA. 2001; 98:5116–5121. [PubMed: 11309499]
46. Kaneko M, Hall JC. Neuroanatomy of cells expressing clock genes in *Drosophila*: transgenic manipulation of the period and timeless genes to mark the perikarya of circadian pacemaker neurons and their projections. J. Comp. Neurol. 2000; 422:66–94. [PubMed: 10842219]
47. Klarsfeld A, et al. Novel features of cryptochrome-mediated photoreception in the brain circadian clock of *Drosophila*. J. Neurosci. 2004; 24:1468–1477. [PubMed: 14960620]
48. Kishiro Y, Kagawa M, Naito I, Sado Y. A novel method of preparing rat-monoclonal antibody-producing hybridomas by using rat medial iliac lymph node cells. Cell Struct. Funct. 1995; 20:151–156. [PubMed: 7641297]
49. Shafer OT, Rosbash M, Truman JW. Sequential nuclear accumulation of the clock proteins period and timeless in the pacemaker neurons of *Drosophila melanogaster*. J. Neurosci. 2002; 22:5946–5954. [PubMed: 12122057]
50. Houl JH, Ng F, Taylor P, Hardin PE. CLOCK expression identifies developing circadian oscillator neurons in the brains of *Drosophila embryos*. BMC Neurosci. 2008; 9:119. [PubMed: 19094242]

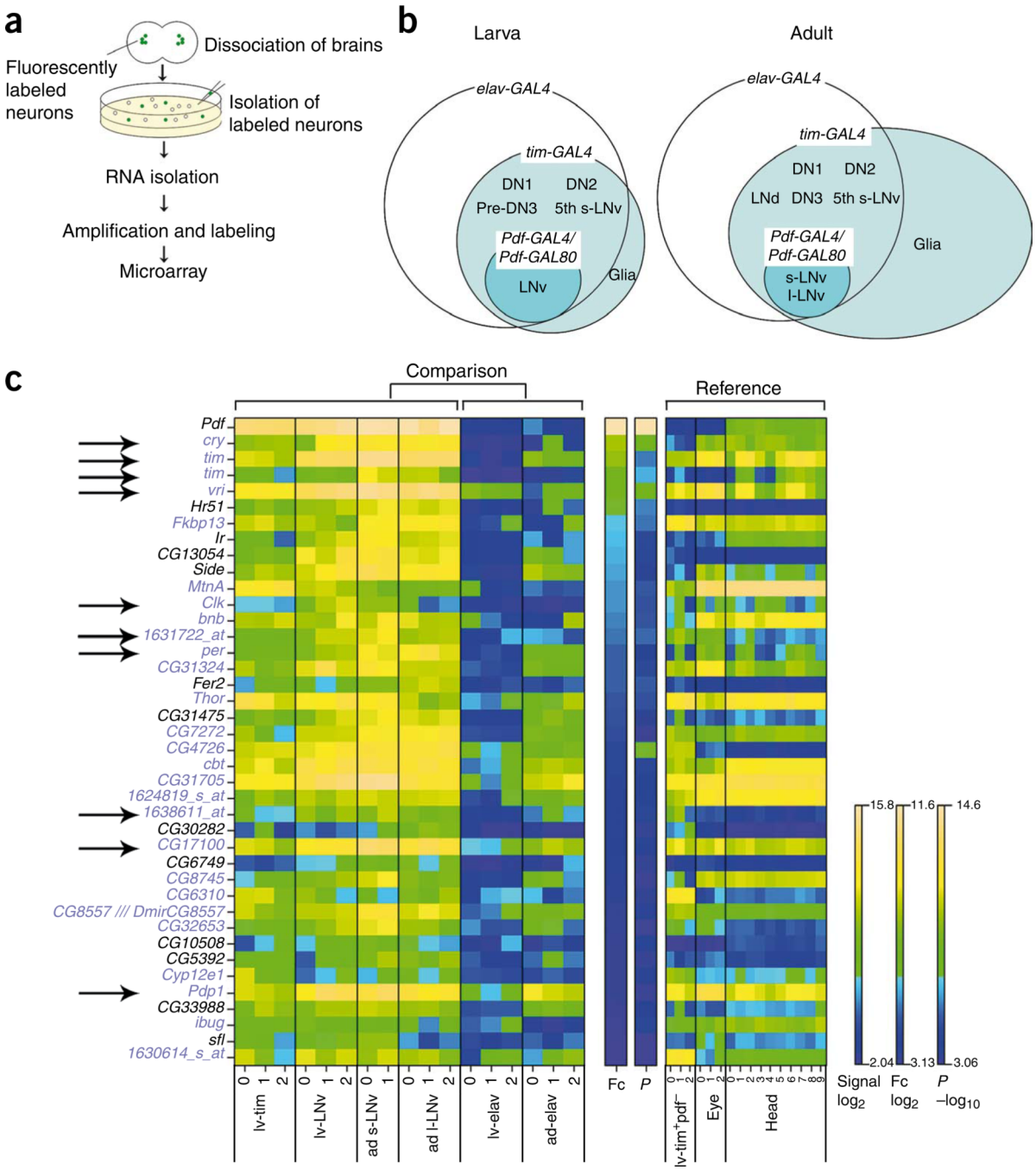

Figure 1.

Gene expression profiling of clock cells in the *Drosophila* brain. (**a**) Strategy of the cell type–specific expression profiling. (**b**) GAL4 and GAL80 drivers used to label clock cells. Left, expression of the drivers in the third-instar larval brain. Right, expression in the adult brain. 5th s-LNv, also known as PDF-negative s-LNv. (**c**) Microarray data for mRNAs enriched in clock cells (see text). Except for head data, 0 to 2 indicate independent replicates. lv, larval; ad, adult; head, heads of wild-type flies collected at different time points. Head data series: 0 and 4 (independent replicates) are ZT3; 5 is ZT7; 1 and 6 are ZT11; 2 and 7 are ZT15; 8 is ZT 19; and 3 and 9 are ZT23. Left panel, data sets used for

comparison and ranking. Middle columns, fold change (Fc) and *t*-test *P*-values. Right panel, data sets used as reference. Top 40 genes (out of 84) that satisfied $P < 0.001$ and $Fc > 8$ are shown (false discovery rate, 1.42%). Scale bars: $\log_2$ of the signal level, $\log_2$ of the fold change, and *P*-value $-(\log_{10})$. Arrows, probe sets for known clock genes; blue probe set names, bona fide pan-clock cell–enriched mRNAs, which are also more highly expressed in the lv-tim$^+$pdf$^-$ cells and the eye than in elav cells; black probe set names, mRNAs that are not highly expressed in lv-tim$^+$pdf$^-$ cells.

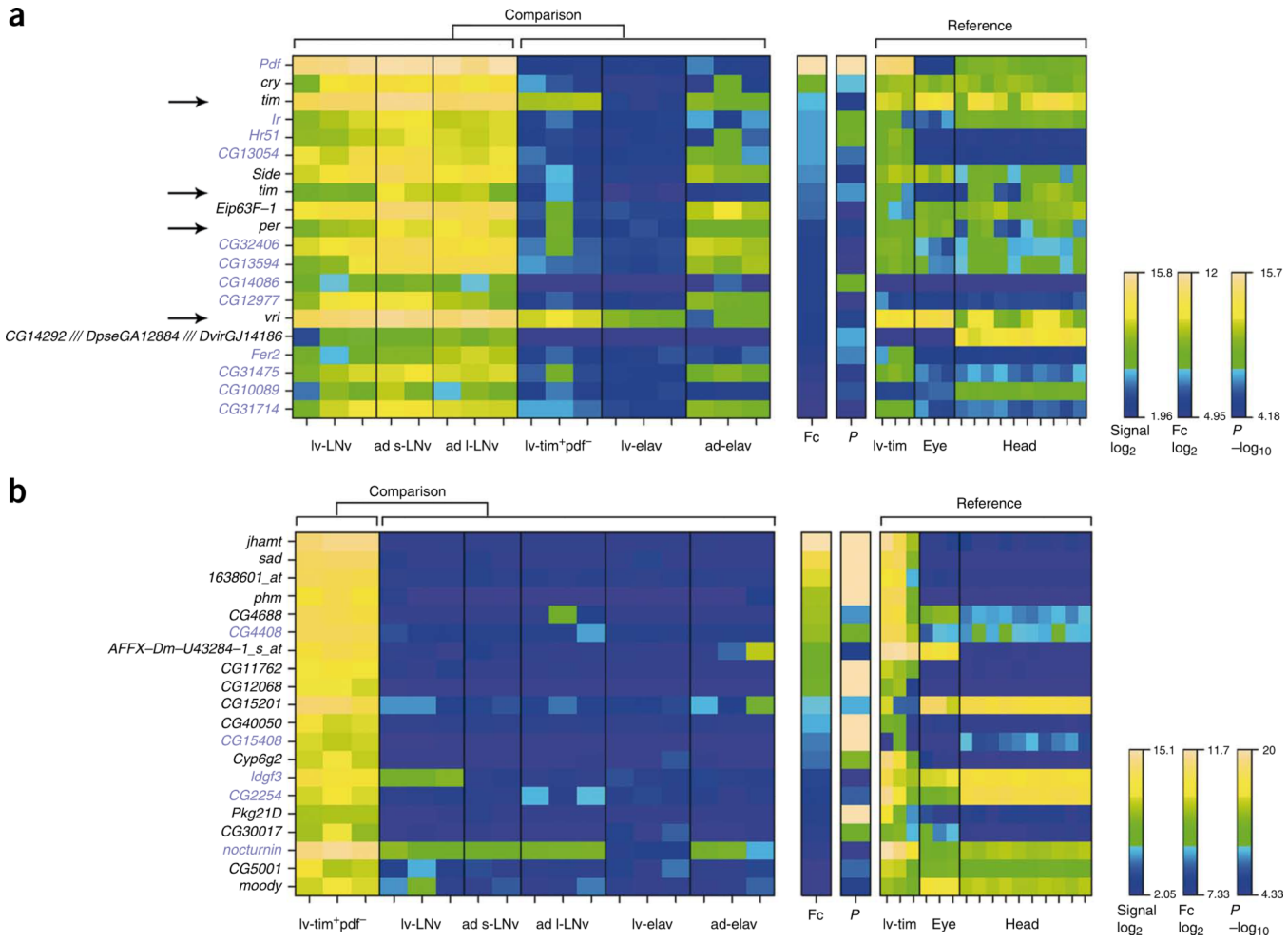

Figure 2.

mRNAs enriched in the subclasses of circadian neurons. (**a**) mRNAs enriched in the PDF-positive LNvs. Microarray data sets from PDF-positive cells and PDF-negative cells (lv-tim^{+}pdf^{-}, lv-elav and ad-elav cells) were compared and ordered by the fold difference from high to low (left). Data sets from other cell types are used as references (right). Top 20 genes that satisfied $P < 0.0001$ and Fc > 8 in this category are shown (false discovery rate, 0.30%). Figure descriptions as in Figure 1c. Arrows, known clock genes; blue probe sets names, bona fide LNv-enriched mRNAs, which are expressed at low abundance in the eye. (**b**) Top 20 mRNAs enriched in lv-tim^{+}pdf^{-} cells. Microarray data from tim^{+}pdf^{-} cells were compared to the average of PDF-positive cells (lv- LNv, adult s-LNv, adult l-LNv), lv-elav cells and ad-elav cells and ordered by the fold difference from high to low ($P < 0.0001$ and Fc > 8, false discovery rate 0.61%) (left). Data sets from other cell types are used as references (right). Blue probe sets names, candidate mRNAs enriched in tim^{+}pdf^{-} cells throughout all developmental stages. These probe sets are also modestly expressed in the heads but at lower abundance in the eye (tim^{+}pdf^{-} > heads > eye).

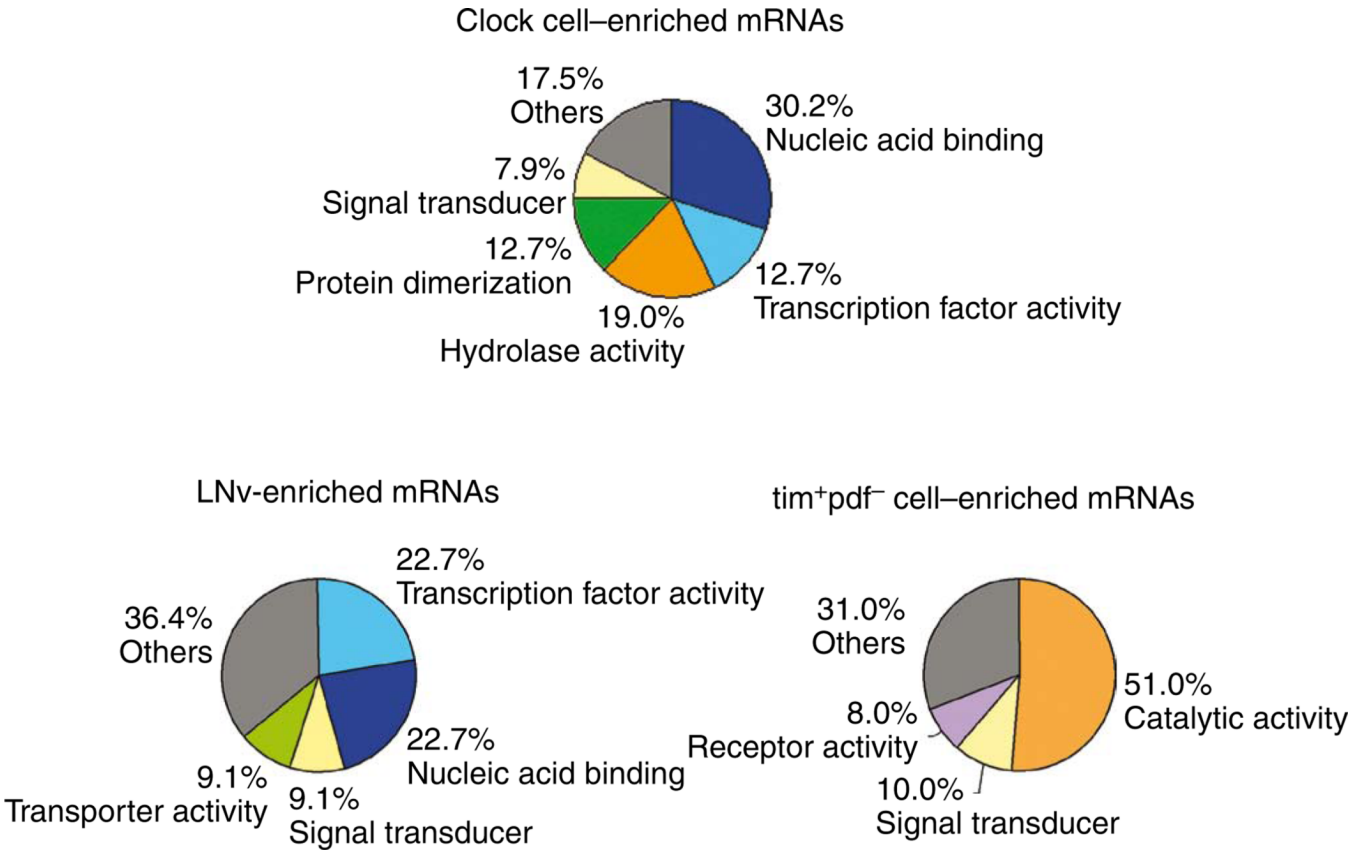

Figure 3.
Functional classifications of the mRNAs enriched in the clock neurons. The genes were assigned to functional classes on the basis of the gene ontology annotation.

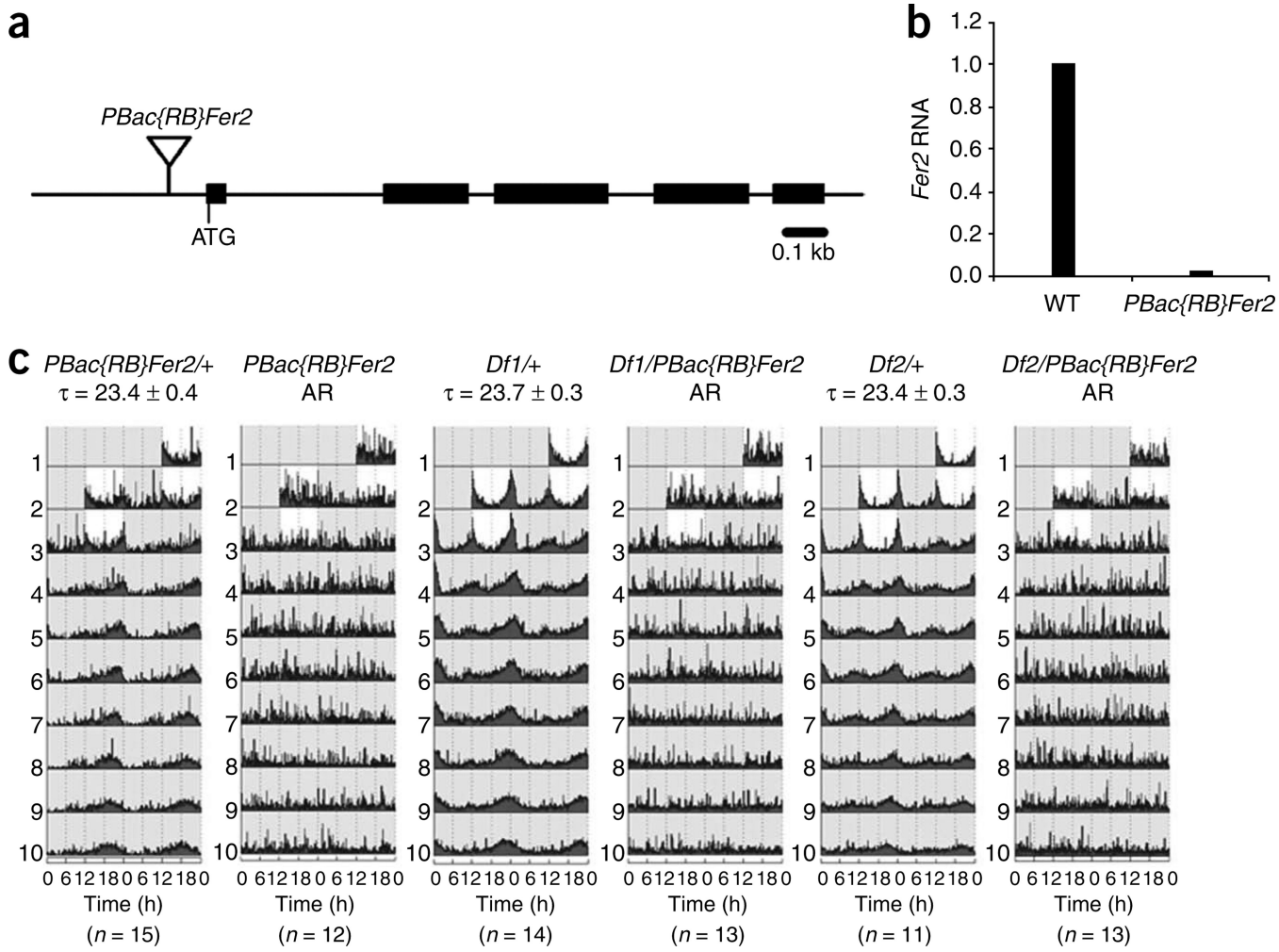

Figure 4.

Fer2 expression is required for behavioral circadian rhythms. (**a**) *Fer2* gene locus. *PBac{RB}Fer2* has a P-element insertion ~100 nucleotides upstream of the first ATG of the *Fer2* ORF. The 5′ and 3′ UTR of *Fer2* are not yet annotated. (**b**) *PBac{RB}Fer2* expresses very little *Fer2* RNA. Amounts of *Fer2* RNA relative to the housekeeping gene *elongation factor 1*β (*Ef1b*) in control embryos (*y w*, wild-type) and *PBac{RB}Fer2* embryos were assayed by real-time PCR. *Fer2/Ef1b* ratio from *PBac{RB}Fer2* is normalized to the value in the control. (**c**) Loss of *Fer2* gene expression disrupts behavioral circadian rhythms. Flies were entrained in 12 h light (white):12 h dark (gray) (LD) for 3 d and released into DD for 10 d. AR, arrhythmic; τ, period length. Double-plotted actograms (activity of two consecutive days shown in one row) of average locomotor activity of flies from the second day in LD to seventh day in DD. Heterozygous *Fer2* mutants (*PBac{RB}Fer2/+*) and heterozygous chromosome 3 deletions (*Df1/+*, *Df2/+*) showed rhythmic locomotor activity in LD and DD, whereas homozygous *Fer2* mutants (*PBac{RB}Fer2*) and hemizygous *Fer2* mutants (*Df1/PBac{RB}Fer2*, *Df2/PBac{RB}Fer2*) were arrhythmic in both LD and DD.

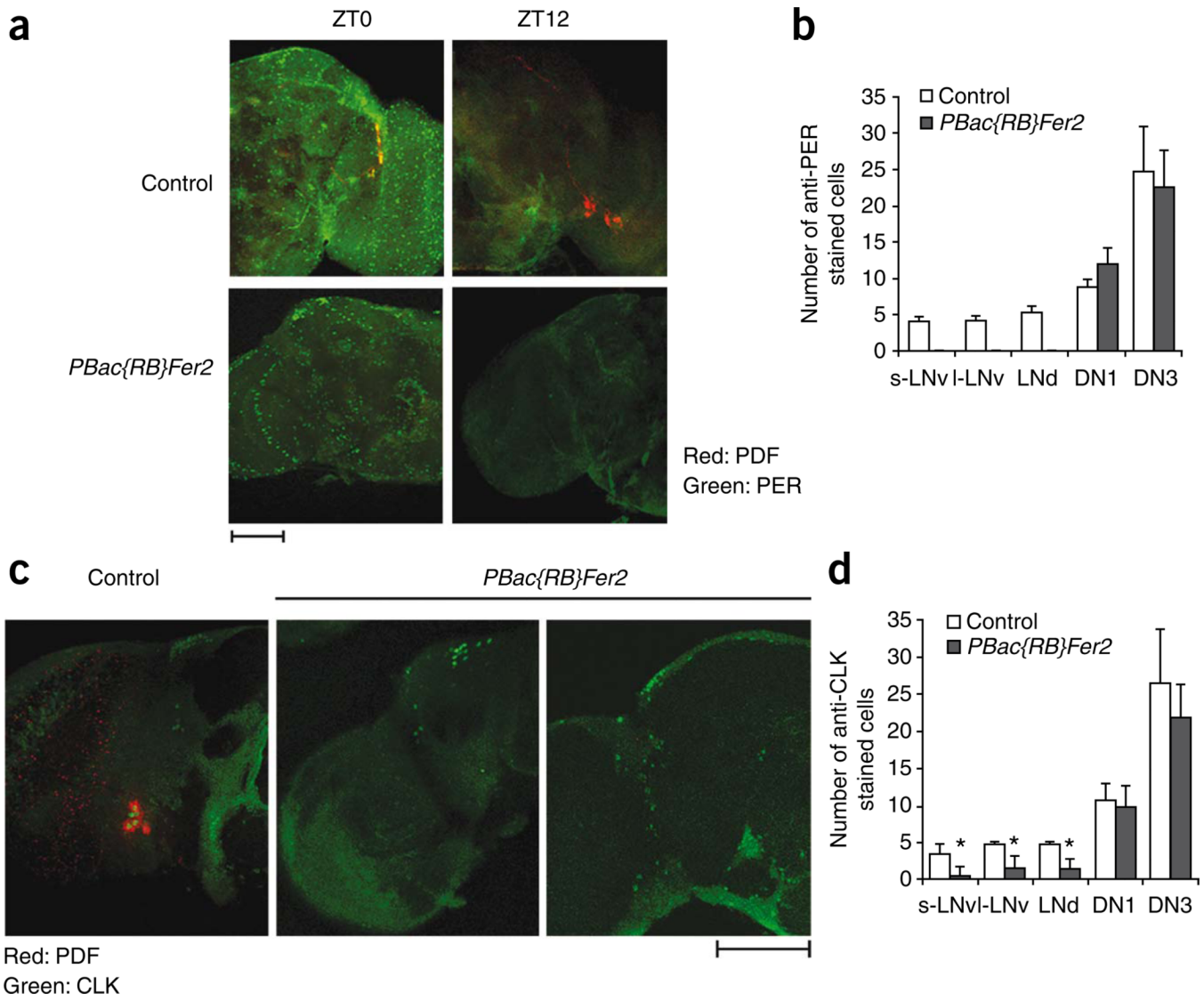

Figure 5.

The *Fer2* gene is required for the specification of the lateral neurons. (**a**) PDF and PER expression in the lateral neurons is abolished in the *Fer2* mutant brain. Homozygous *PBac{RB}Fer2* and control (heterozygous) fly brains were collected at ZT0 and ZT12, and PER and PDF were detected as described in Online Methods. *z*-stack projections of confocal images are shown. Scale bar, 100 μm. (**b**) Quantification of PER-positive cells in the brains at ZT0 (peak time for PER accumulation). A minimum of seven brain hemispheres were analyzed. At ZT12, none of the clock neurons showed PER immunoreactivity. (**c**) Representative staining results of CLOCK (CLK) in control and *Fer2* mutant brains. Fly heads were collected at ZT22 and immunostained with anti-CLK and anti-PDF. *Fer2* mutant brain has detectable yet fewer CLK-stained cells. Scale bar, 100 μm. (**d**) Quantification of CLK-positive cells in the *Fer2* mutant and control brains. Six brains of control and ten brains of the mutant were analyzed. There were significantly fewer CLK-positive s-LNvs, l-LNvs and LNds in mutant than in control (*$P < 0.001$, two-sample *t*-test; error bars, s.d.).

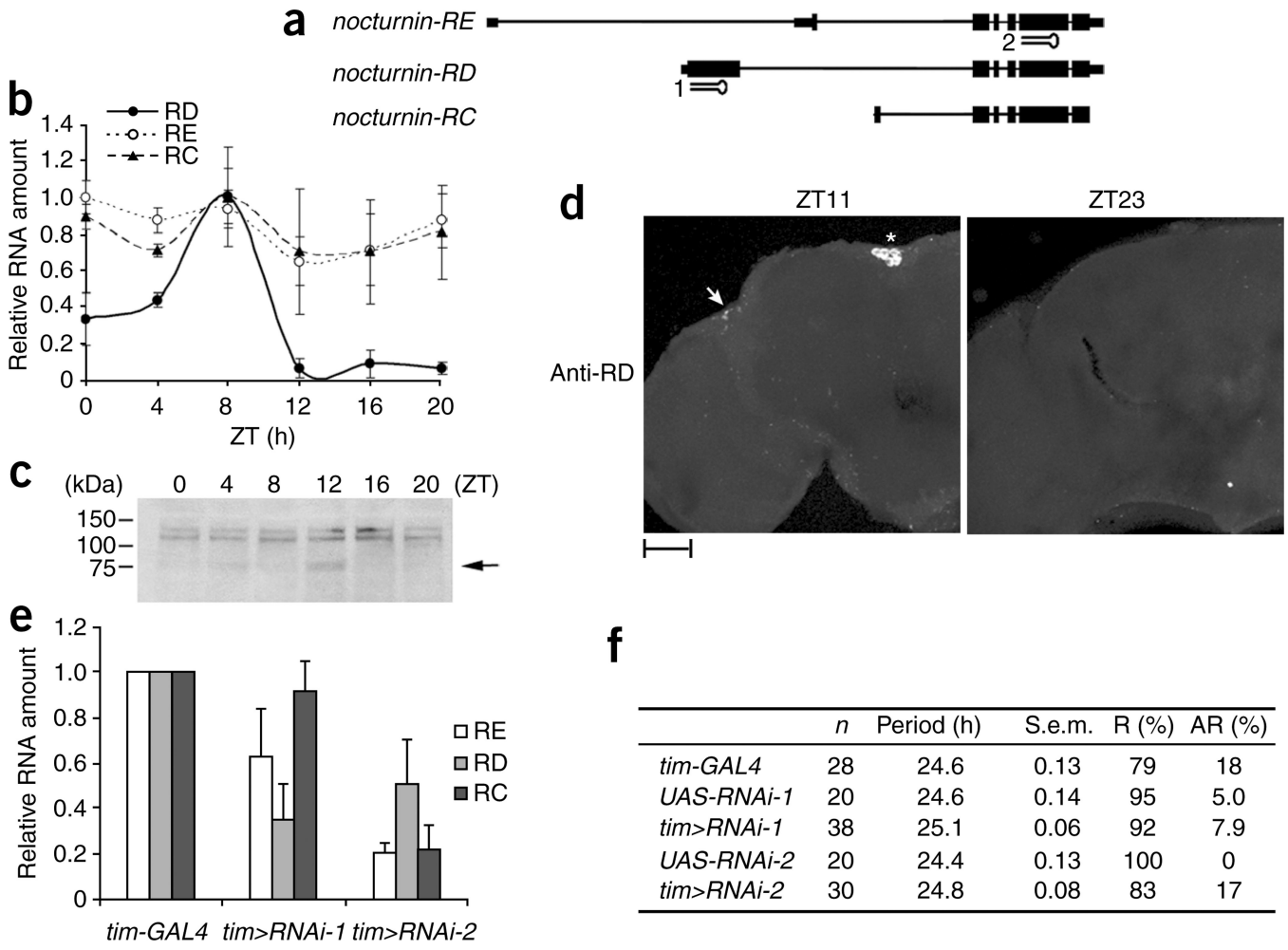

f

	n	Period (h)	S.e.m.	R (%)	AR (%)
tim-GAL4	28	24.6	0.13	79	18
UAS-RNAi-1	20	24.6	0.14	95	5.0
tim>RNAi-1	38	25.1	0.06	92	7.9
UAS-RNAi-2	20	24.4	0.13	100	0
tim>RNAi-2	30	24.8	0.08	83	17

Figure 6.

nocturnin-RD is rhythmically expressed in a subset of clock neurons. (**a**) *nocturnin* gene and the RNAi target sites. Hairpin 1, *UAS-RNAi-1*. Hairpin 2, *UAS-RNAi-2*. (**b**) Relative RNA abundance of the *nocturnin* isoforms in wild-type fly heads. Head RNA collected at six time points was analyzed by real-time PCR using the primer pair specific for each isoform, normalized by the abundance of *Ef1*β RNA. (**c**) NOC-RD expression shows daily rhythms. Protein extract of the wild-type fly heads collected at six time points in LD was analyzed by western blotting with anti-RD. Arrow, NOC-RD at the predicted molecular weight (71.9 kDa). (**d**) NOC-RD expression in the adult brain. *y w* fly brains were collected at ZT11 and ZT23 and immunolabeled with the RD-specific monoclonal antibody. Arrow, dorsal neurons detected by anti-RD; asterisk, nonspecifically labeled cells. Scale bar, 50 μm. (**e**) Efficiency of *nocturnin* RNAi, measured by RNA abundance. *tim-GAL4* or *tim-GAL4,UAS-RNAi* flies were collected at ZT5, and the RNA abundance of each *nocturnin* isoform relative to *Ef1*β RNA in the heads was analyzed by real-time PCR. *nocturnin/Ef1b* ratios from the knockdown lines were normalized to the *tim-GAL4* line value. Two or three independent samples were analyzed. Error bars, s.d. (**f**) Free-running behavior rhythms of the *nocturnin* RNAi flies in DD. *tim>RNAi-1* (*tim-GAL4, UAS-RNAi-1*) targets RD isoform. *tim>RNAi-2* (*tim-GAL4, UAS-RNAi-2*) efficiently knocks down RE and RC isoforms. Detailed genotypes used for the behavior assay are described in Online Methods. Flies were entrained in 12 h:12 h LD for 3 d and released in DD for 10 d. R, rhythmic; AR, arrhythmic.

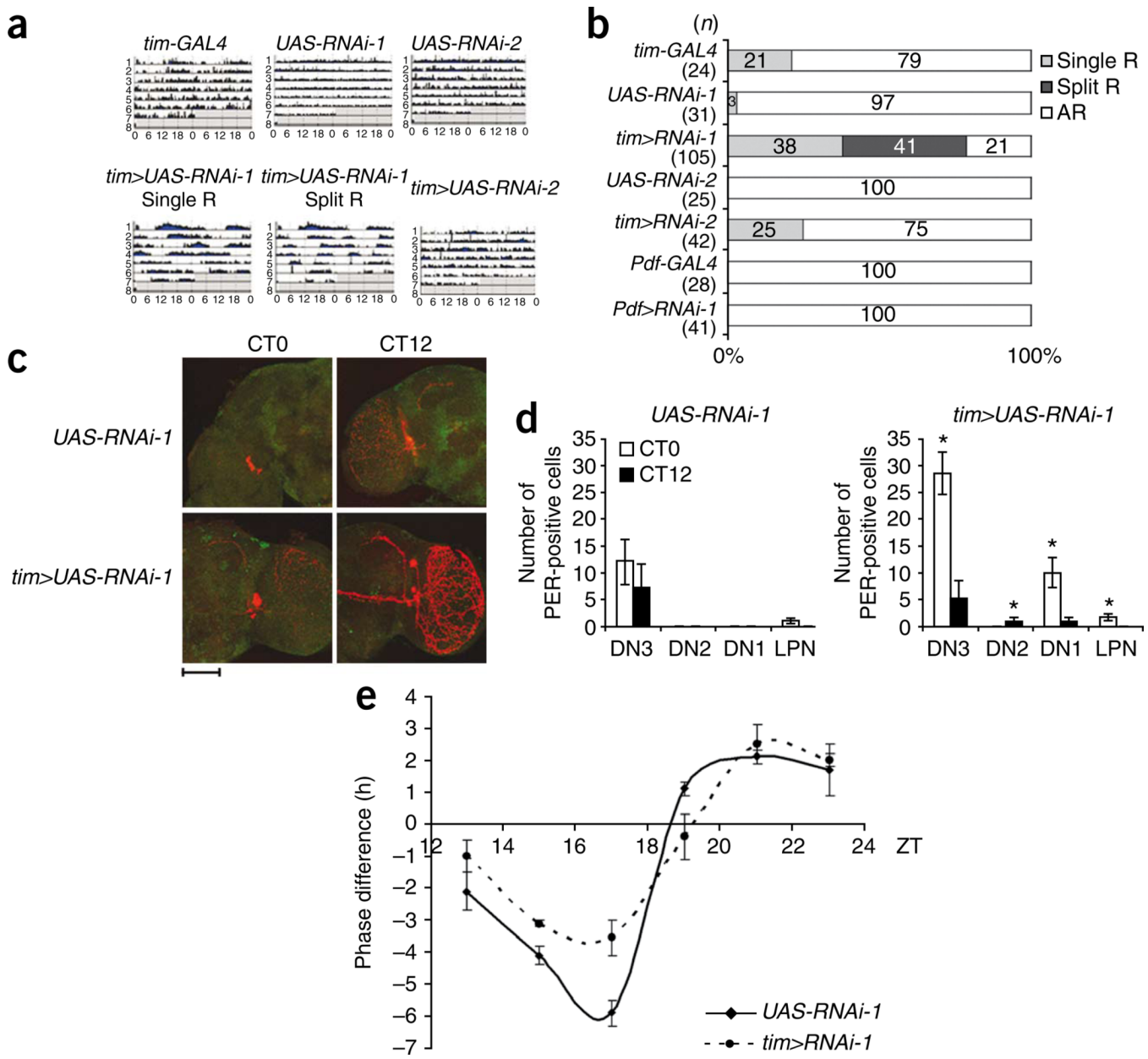

Figure 7.

NOCTURNIN mediates light-mediated behavioral response in dorsal neurons. (**a**) Representative double-plotted actograms of the behavior rhythms in constant light (LL). Flies were entrained in LD for 3 d and released in LL for 9 d. Single R, locomotor activity with single rhythmic component; split R, complex rhythms with short and long components. (**b**) Results of the locomotor assay in LL. Detailed genotypes used for the assay are described in Online Methods. Graph depicts the percentages of the flies that were arrhythmic in LL (white), that showed single rhythms (gray) and that had split rhythms (black). (**c**) PER expression in LL. Control flies (*UAS-RNAi-1*) and *nocturnin-RD* knockdown flies (*tim>UAS-RNAi-1*) were entrained in LD and released in LL. Brains were collected during the fourth day in LL (LL4) at CT0 (circadian time 0, subjective dawn) and CT12 (subjective dusk), and PER (green) and PDF (red) expression were examined by immunostaining. Scale bar, 100 μm. (**d**) Quantification of PER-positive cells at LL4. PER

expression in DN1, DN3 and LPN cells cycled in the *nocturnin-RD* knockdown flies, whereas there were much fewer PER immunoreactive cells in the control brain and no significant change in numbers between two time points (*$P < 0.05$, two-sample *t*-test; error bar, s.d.). (**e**) Phase response curves of the control and *nocturnin-RD* knockdown flies: *x* axis, time of the light pulse (ZT, h); *y* axis, phase change (±h). Averages of two independent experiments. Negative values, phase delays; positive values, phase advances. Error bar, s.e.m.